

NASA TECHNICAL NOTE



NASA TN D-2150

C. 1

LOAN COPY: RETD
AFWL (WLIL-
KIRTLAND AFB, N



NASA TN D-2150

EXPLORER VIII SATELLITE MEASUREMENTS IN THE UPPER IONOSPHERE

by R. E. Bourdeau and J. L. Donley
Goddard Space Flight Center
Greenbelt, Maryland



EXPLORER VIII SATELLITE MEASUREMENTS
IN THE UPPER IONOSPHERE

By R. E. Bourdeau and J. L. Donley

Goddard Space Flight Center
Greenbelt, Maryland

NATIONAL AERONAUTICS AND SPACE ADMINISTRATION

For sale by the Office of Technical Services, Department of Commerce,
Washington, D.C. 20230 -- Price \$0.75

EXPLORER VIII SATELLITE MEASUREMENTS IN THE UPPER IONOSPHERE

by

R. E. Bourdeau and J. L. Donley

Goddard Space Flight Center

SUMMARY

This is a more extensive report than earlier ones on upper ionospheric ion composition (Bourdeau et al., 1962) and electron temperature (Serbu et al., 1961) and on spacecraft-plasma interaction (Bourdeau et al., 1961), all measured by use of Explorer VIII.

Results from an ion-retarding-potential experiment show that the upper ionospheric composition responds to the neutral gas temperature. Specifically, during the satellite's active life (November-December, 1960), O^+ ions predominated from perigee (425 km) up to about 800 km at night and 1500 km at diurnal maximum; the base of the helium ion region was located at 800 km during the sunrise period and at 1500 km in the daytime; the base of the protonosphere possibly was located at 1200 km during the sunrise period and above 1800 km at diurnal maximum.

For the latitudes indicated, the electron temperature (T_e) data—restricted herein to magnetically quiet days ($A_p < 15$)—are consonant with current models of the diurnal electron density behavior and with a hypothesis of solar ultraviolet radiation as the only ionizing agent. For the 6-hour period centered at midnight, the average T_e observed at altitudes 425-600 km was 900°K with a standard deviation of 150°K. There were no anomalously high values and no significant change with magnetic dip (0° - 75° N). For the period 10-16 hours LMT, at magnetic dips between 50° - 70° S and at altitudes between 1000-2400 km, the observed average T_e was 1600°K with a standard deviation of 200°K when a small percentage of anomalously high values are excluded. The most pronounced feature of the measured diurnal variation is that T_e exceeds the neutral gas temperature by a factor of about 2.5 during the sunrise period in the altitude region 600-900 km. Explanations are suggested for differences between the Explorer VIII T_e observations and other ground-based and spaceflight measurements of upper ionospheric parameters.

The measured satellite-plasma interaction is consistent with theory, lending confidence to the geophysical results described above. The observed "average" satellite potential varied from a few tenths of a volt negative at night, to zero when the measured daytime charged particle density was 10^4 cm^{-3} and thence to a few tenths of a volt positive for daytime densities of 10^3 cm^{-3} . Superimposed on the "average" potential were experimentally observed potential gradients across the satellite skin—an effect produced by the movement of a conducting body through a magnetic field. The measured orientation sensitivity of three types of current flowing between the satellite and the ionosphere is described.

CONTENTS

Summary	i
INTRODUCTION	1
THE POTENTIAL OF THE EXPLORER VIII SATELLITE.....	3
MEASUREMENTS OF PLASMA-TO-SATELLITE ION CURRENT	5
MEASUREMENTS OF PLASMA-TO-SATELLITE ELECTRON CURRENT	7
ELIMINATION OF INTERACTION EFFECTS IN DERIVING GEOPHYSICAL PARAMETERS	10
SUMMARY OF ION COMPOSITION RESULTS	10
SUMMARY OF ELECTRON TEMPERATURE RESULTS	13
References	17

EXPLORER VIII SATELLITE MEASUREMENTS IN THE UPPER IONOSPHERE

by

R. E. Bourdeau and J. L. Donley
Goddard Space Flight Center

INTRODUCTION

The Explorer VIII Satellite was devoted primarily to the measurement of upper ionospheric parameters by environmental sampling techniques. Prior to this satellite launching, the ionosphere had been studied mainly by classical ground-based and rocketborne radio-propagation methods. The success of environmental sampling methods depends on evaluation of the interactions between a spacecraft and the surrounding ionized medium. The relative sparsity of spaceflight observations on the interaction phenomena dictated (1) that the spacecraft configuration be as simple as possible and (2) that it carry supporting experiments designed specifically to study the interaction and thus permit valid interpretation of the geophysical data.

The interaction was minimized by restricting the use of protuberances, by foregoing the use of solar cells and so maintaining an equipotential surface, and by limiting the telemetry transmitter power to a value which previous results showed would not seriously affect the vehicle potential. These factors proved advantageous in that the studied interaction is quite explainable from kinetic theory considerations as applied to satellites (Gringauz and Zelikman, 1957), thus lending confidence to the reported ionospheric parameters. However, the limited active life together with the nature of real time telemetry transmissions and the scarcity of receiving sites able to accept the low signal levels restricted the acquired data to specific latitude, altitude and temporal conditions.

The satellite was launched on November 3, 1960, into an orbit with a 50° equatorial inclination, a perigee of 425 km, and an apogee of 2400 km. The planned active life was two months. The spacecraft (Figure 1) consisted of two truncated cones joined at the equator. Thermal coatings were placed on both cones in a pattern designed to maintain an equipotential surface. The spin rate at injection was reduced to an orbital value of 22 rpm so that retarding potential curves could be obtained for a minimum orientation change. Of the ten experiments, six are pertinent to this report.

Two different but gratifyingly redundant electron temperature sensors were located near the forward end of the spin axis. One of these also provided data on the ambient electron density, the average potential ϕ_0 of the satellite, and the behavior of the electron current i_e from medium to satellite as a function of position relative to the velocity vector. This electron temperature sensor is visible in Figure 1; the other was diametrically opposite. The remaining four sensors were on

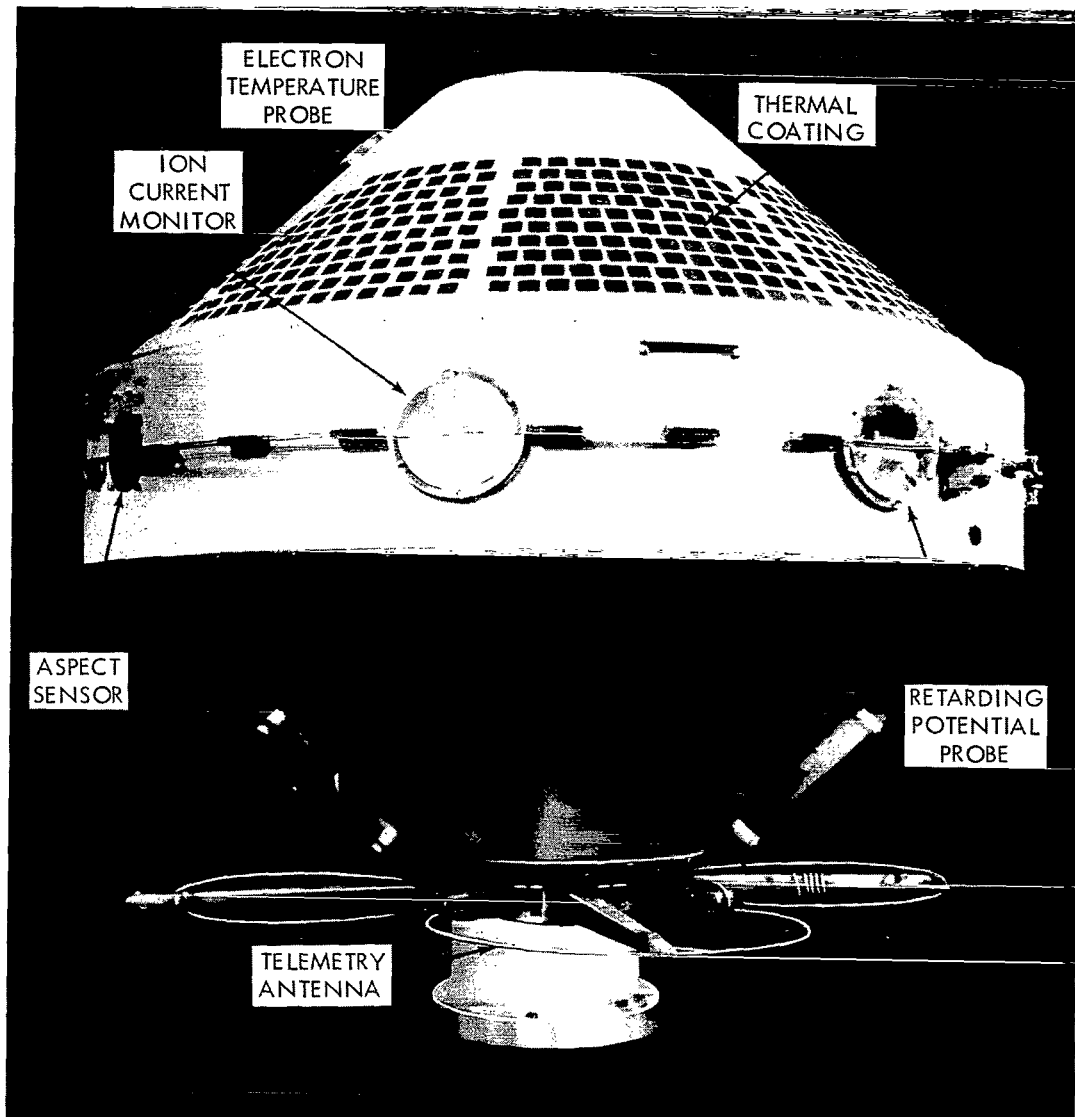


Figure 1—The Explorer VIII satellite.

the satellite's equator; two are seen in Figure 1 and the other two are diametrically opposite. One of these was a retarding potential analyzer designed to measure ion composition. The second measured the positive ion current i_+ from medium to satellite as a function of position relative to the velocity vector. The third measured the sum of i_e and the photocurrent i_p . A comparison of the output of this sensor, when not oriented toward the sun, with the i_e measurement made near the forward end of the spin axis reveals the behavior of i_e as a function of magnetic field orientation. The fourth experiment provided redundancy by measuring the sum of i_e , i_+ and i_p , or the total current exchange between the spacecraft and the ionosphere.

THE POTENTIAL OF THE EXPLORER VIII SATELLITE

The "average" potential of a conducting body at rest where RF and magnetic fields and solar radiation may be neglected is given by

$$\phi_0 = - \frac{kT_e}{e} \ln \frac{J_e}{J_+} \quad (1)$$

where k is Boltzmann's constant, e is the electronic charge, and J_e and J_+ are the respective electron and ion current densities in the undisturbed ionosphere. On the assumption of temperature and charge equilibrium between electrons and ions ($T_e = T_+$, $n_e = n_+$), this reduces to:

$$\phi_0 = - \frac{kT_e}{e} \ln \frac{(m_+)^{1/2}}{(m_e)^{1/2}} \quad (2)$$

where m_+ and m_e are the respective ion and electron masses. In a medium containing only O^+ ions at a temperature of $1000^\circ K$, the computed potential is -0.44 volt.

In the practical case of a conducting body moving with satellite velocity through the nighttime ionosphere, the average potential (again neglecting the effects of RF and magnetic fields) is given by:

$$\phi_0 = - \frac{kT_e}{e} \ln \frac{\int J_e dS_e}{\int J_+ dS_+} \quad (3)$$

where S_e and S_+ are the areas over which the respective electron and ion currents are effective. It can be shown that this reduces approximately to

$$\phi_0 \approx - \frac{kT_e}{e} \ln \frac{v_e}{V} \quad (4)$$

where v_e and V are the respective electron and satellite velocities. For $T_e = 1000^\circ K$, the computed average potential is approximately -0.29 volt. This is to be compared with measured Explorer VIII nighttime average potential values between -0.5 and -0.75 volt for the electron temperature indicated. This is an improvement by an order of magnitude in the agreement between measured and predicted satellite potentials over that obtained by other investigators, specifically Krassovsky (1959) who reported negative potentials up to 6 volts from Sputnik III. Factors which might contribute to the difference between predicted and observed Explorer VIII nighttime potentials are the presence of RF and magnetic fields—which are not taken into account in Equation 4, and thus affect the predicted result—and a contact potential which can influence the experimental value. The rectification effect of the antennas used for telemetry transmissions would tend to make the vehicle potential more negative than that computed from Equation 4. The Japanese work (Aono et al., 1962) on resonance probes demonstrates that if the frequency of RF transmissions exceeds the plasma frequency the effect should be small. Whale (1963), on the other hand, points out that this is so only for low values of RF power. It is possible, therefore, from the work of other investigators to show

qualitatively that a large increase in potential would not be expected for the amount of power (100 mw) and the frequency (108 Mc) used by the Explorer VIII telemetry system. However, these other data are not quantitative enough to permit a categorical statement that an increase of a few tenths of a volt—which is the difference between the predicted and observed Explorer VIII values—is not possible from the RF rectification effect. The earth's magnetic field can affect the electron diffusion current preferentially. However, for the Explorer VIII form factor and orbit considered here, E. C. Whipple, Jr. (private communication) computes a negligible effect of the magnetic field on the average satellite potential. Another possibility is an unknown in the measurement of the spacecraft potential. This measurement, described in detail in a later section, depends on the assumption that the aperture electrode of the measuring instrument is at the same potential as the adjacent satellite skin. Possible differing work functions could result in different surface contact potentials and consequently introduce an error in the measurement.

Consider now the more complicated case of daytime satellite potentials. Solar radiation causes electrons to be emitted from the satellite surface in such a way that

$$\phi_0 = - \frac{kT_e}{e} \ln \frac{\int J_e dS_e}{\int J_+ dS_+ + \int J_p dS_p} \quad (5)$$

For the altitudes considered here, the photocurrent effect $\int J_p dS_p$ masks the ion diffusion effect $\int J_+ dS_+$ and thus competes with electron diffusion $\int J_e dS_e$ for the determination of the polarity of the satellite potential. For an orientation where the sun shines directly on the satellite's equator, S_e

is approximately $4 \times S_p$. The observed magnitude from Explorer VIII of J_p is 5×10^{-9} amps cm^{-2} (Bourdeau et al., 1961), a value independent of altitude for the particular orbital elements. This is to be compared with a value of 2.3×10^{-9} amps cm^{-2} previously measured by Hinteregger et al. (1959) on a rocket at a lower altitude. The transition from a negative to a positive satellite potential for the Explorer VIII case can be predicted to occur when $4 J_e = en_e v_e = 5 \times 10^{-9}$ amps cm^{-2} . For $T_e = 1000^\circ \text{K}$, it is predicted that the polarity of the satellite potential will reverse for $10^3 \text{ cm}^{-3} < n_e < 10^4 \text{ cm}^{-3}$. This is consistent with our observations that the average daytime Explorer VIII potential was approximately -0.15 volts for $n_e \approx 10^4 \text{ cm}^{-3}$ and a few tenths of a volt positive at apogee when $n_e \approx 10^3 \text{ cm}^{-3}$.

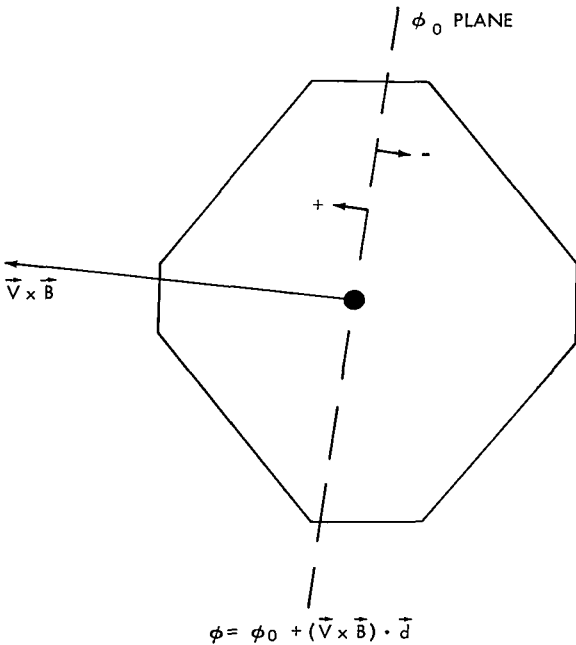


Figure 2—The induced emf effect.

The motion of the satellite with velocity \vec{V} through the magnetic field \vec{B} produces an induced potential that is a function of position on the satellite surface,

$$\phi = \phi_0 + (\vec{V} \times \vec{B}) \cdot \vec{d} \quad (6)$$

where \vec{d} is the vector distance of any point on the surface from the satellite center. A satellite potential of ϕ_0 will be measured at all points that lie on a plane through the satellite center perpendicular to $\vec{V} \times \vec{B}$. All other points will be more positive or negative than ϕ_0 as they are situated on one side of this plane or the other (Figure 2). The measurement (Bourdeau et al, 1961) at an altitude of 1000 km shows a potential difference of 0.14 volt across the satellite equator, a value consistent with that computed from Equation 6 using known values of \vec{V} , \vec{B} and \vec{d} .

MEASUREMENTS OF PLASMA-TO-SATELLITE ION CURRENT

The positive ion current i_+ flowing from the ionosphere was monitored by the sensor shown schematically in Figure 3. The inner grid is biased negatively to suppress photoemission from the collector and to remove incoming electron current so that the collector responds only to ions diffusing from the ionosphere.

As the satellite spins, it is possible to plot i_+ as a function of the azimuth angle of the sensor relative to the velocity and solar vectors. A typical example is illustrated in Figure 4. The absence of a current when the sensor is pointed at the sun is proof that photoemission from the collector has been successfully suppressed. The observation that i_+ is zero in the satellite wake is to be expected from the relative satellite and ion velocities and is definite but indirect experimental evidence for an electron sheath immediately adjoining the vehicle at this location.

When the sensor is pointed within 45 degrees of the velocity vector, the observed collector current is given by the equation

$$i_+ = \alpha_+ n_+ A e V \cos \theta, \quad \theta < 45^\circ, \quad (7)$$

where α_+ is the combined electrical transparency of the grids for positive ions, A is the area of the collector and θ the angle between the sensor normal and the satellite velocity vector. A comparison of the measured i_+ from this sensor with that observed on an exposed collector described in a succeeding section shows that the electrical transparency α_+ is equal to the optical transparency (92 percent). Whenever, as in this case, the average satellite potential is negative and v is large compared to the thermal velocity of the ion, the ion collection volume is computed from known parameters and consequently the device provides an accurate measurement of charged particle density. Confidence in this statement is based on the agreement between n_+ values computed from Equation 7 with measured i_+ values

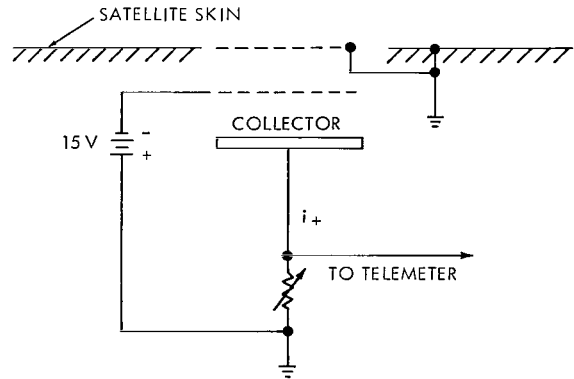


Figure 3—Ion current monitor.

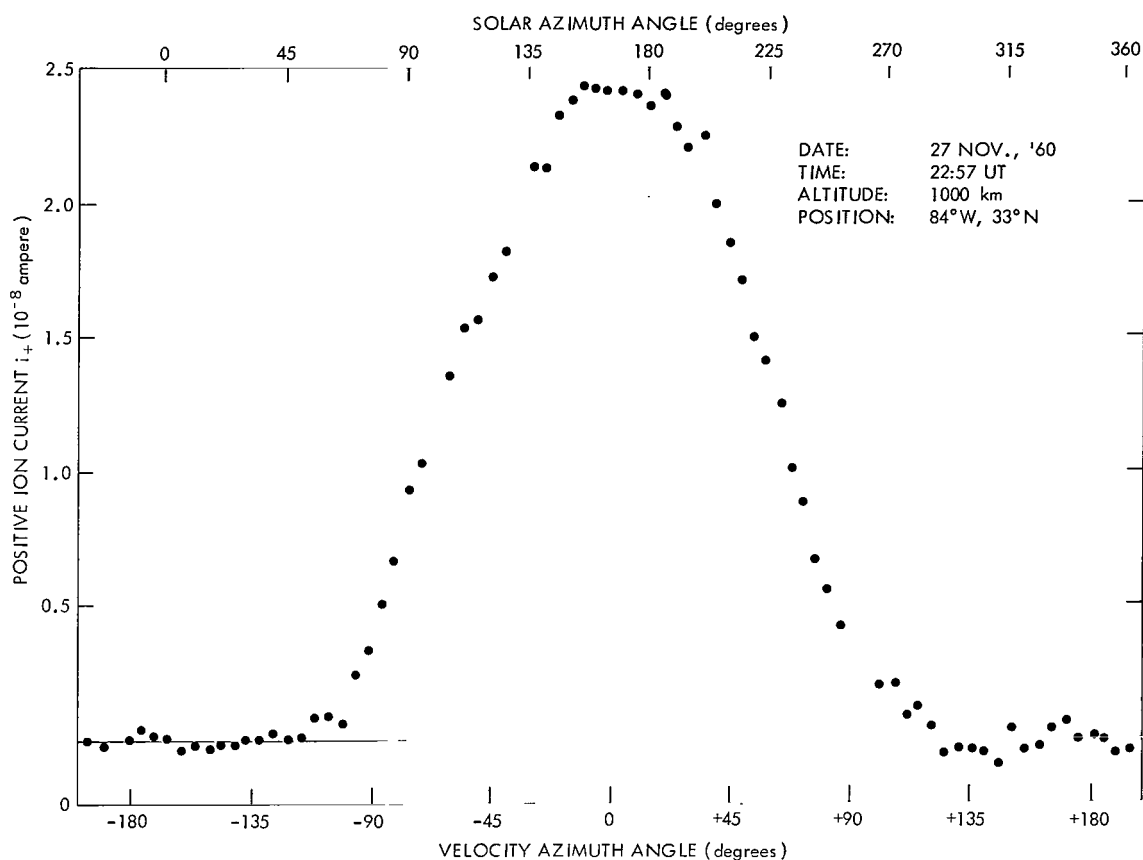


Figure 4—Ion current as a function of aspect.

and electron densities measured by the two-element electron temperature experiment described in a succeeding section. An even better test has been performed by Donley (1963), who shows good agreement between ion densities obtained by a similar experiment on a SCOUT rocket and electron densities simultaneously measured by Bauer and Jackson using radio-propagation methods.

When the angle of the sensor normal relative to the velocity vector is 90 degrees, the observed i_+ should behave as though the body is at rest. Current theory for this condition results in

$$i_+ = \frac{\alpha_+ n_+ A e a}{2\sqrt{\pi}}, \quad \theta = 90^\circ, \quad (8)$$

where a is the most probable thermal velocity of the particle. We find that the observed value for $\theta = 90^\circ$ is larger than what would be computed from Equation 8 for reasonable values of ion temperature. This discrepancy represents a gap in current theories which assume a discrete boundary for the satellite's surrounding ion sheath. The most likely explanation for the difference is that Equation 8 should be modified to account for the effect on the positive ion collection of electric fields penetrating the sheath at the sides of the satellite (Schulz and Brown, 1955). Another possible reason is that factually we are not dealing with the planar geometry for which Equation 8 applies.

MEASUREMENTS OF PLASMA-TO-SATELLITE ELECTRON CURRENT

It can be expected that the electron current diffusing from the ionosphere to satellite would be modulated in accordance with orientation changes relative to both the velocity and magnetic field vectors. It is possible to present measurements of these two effects separately by choosing data obtained at critical satellite orientations. Specifically, we can examine measured electron currents taken at small distances from the ϕ_0 plane (cf. Figure 2) where changes due to the magnetic field effect are not permitted even though the spacecraft is spinning. Data were so obtained by use of the experiment illustrated in Figure 5. The sensor consists of two electrodes, an aperture grid maintained at spacecraft potential, and a collector. The positive bias on the latter serves to exclude the effects of positive ion and of photocurrents, resulting in unambiguous measurements of only the electron diffusion current.

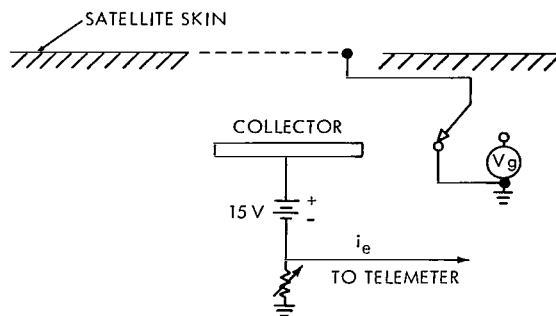


Figure 5—Electron temperature probe.

The result, in the form of a graph of electron current as a function of orientation relative to the velocity vector, taken when the average satellite potential was -0.15 volt, is illustrated in Figure 6. A maximum is observed in the direction of motion and a minimum in the satellite's wake, representing 15 percent more or less, respectively, than that measured for an orientation perpendicular to the velocity vector. This modulation index is explainable to the first order by the ratio of

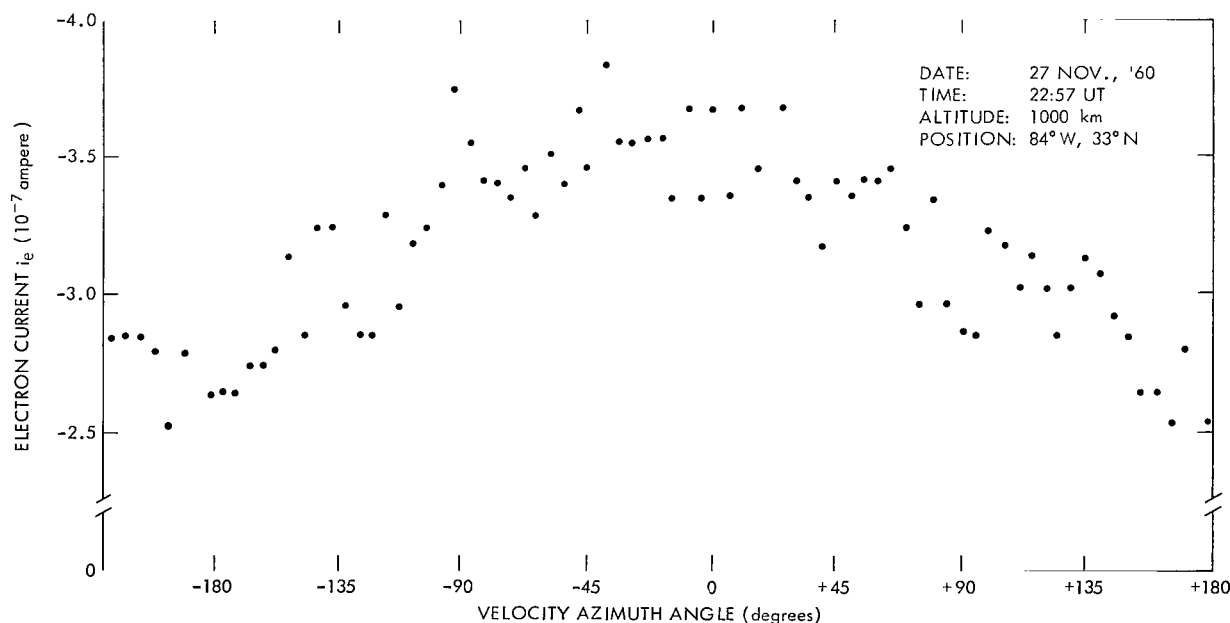


Figure 6—Electron current as a function of aspect.

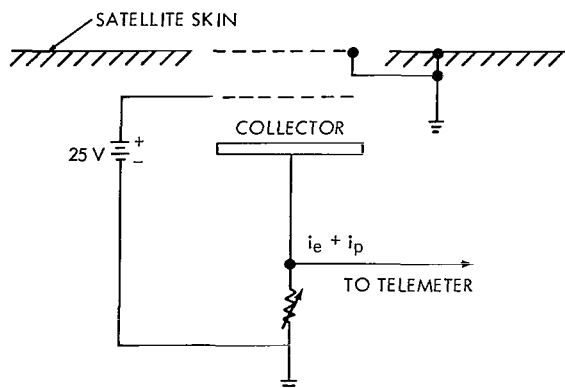


Figure 7—Electron and photocurrent monitor.

situated on the satellite's equator. A schematic of the electron current monitor is illustrated in Figure 7. This sensor responds to photocurrent when pointed toward the sun and to the diffusion of ambient electrons from the ionosphere. The result illustrated in Figure 8 was obtained for an orientation such that magnetic field modulation of the electron diffusion current can be considered minimal. A large photocurrent effect is observed whenever the sensor is oriented within 45 degrees of the sun. Elsewhere it is assumed that we are observing only electron diffusion current. As is expected, this current is a minimum when the sensor is located in the wake. We additionally emphasize (1) that the small percentage modulation is consistent with the relative electron and

electron-to-satellite velocity. The results do contrast with those of Willmore et al. (1962) who report at least an order of magnitude electron current depletion in the wake of the Ariel satellite.

We have considered the possibility that the discrepancy between the aforesaid Explorer VIII and Ariel observations is due to the fact that the data illustrated in Figure 6 were obtained near the forward end of the spin axis and thus represent results taken near the edge of the wake. This consideration involves examining data taken when the spin axis was perpendicular to the velocity vector and obtained by use of an electron current monitor

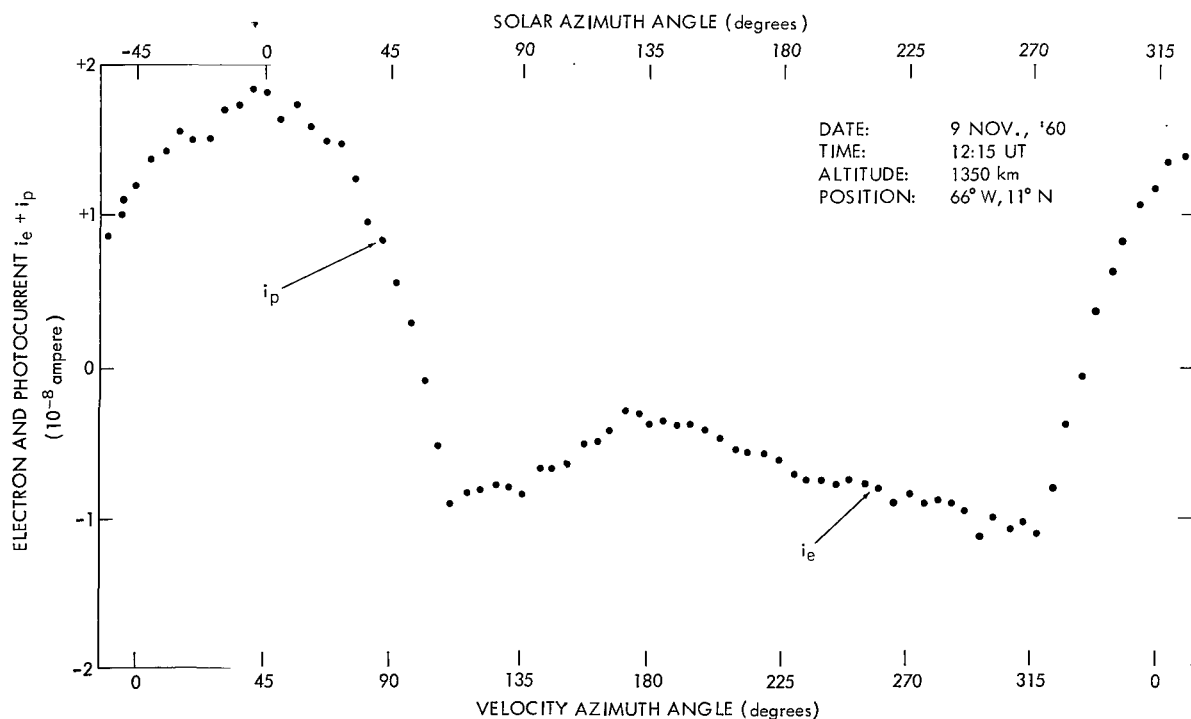


Figure 8—Electron and photocurrent as a function of aspect.

satellite velocities and, (2) that an appreciable current is observed for $\theta = 180^\circ$, when the sensor is extremely close to the *center* of the wake. We still are left with a difference between the Explorer VIII and Ariel results which perhaps is due to the different spacecraft for m factors.

We now can consider magnetic field modulation of the electron diffusion current by examining measured values of total or net current to the satellite surface. This was accomplished by measuring the current to a collector flush with and insulated from the satellite skin (Figure 9). This particular sensor was located on the satellite's equator. A typical daytime result is shown in Figure 10. Three pronounced effects are evident: (1) the peak ram ion current as the sensor most nearly points in the direction of motion; (2) the masking photocurrent as the sensor points to the sun; and (3) the maximum electron current when $\theta \approx 280^\circ$. It is the latter observation which illustrates magnetic field modulation of the electron current. A previous analysis (Bourdeau et al., 1961) shows that this maximum occurs exactly when the azimuth angle between the sensor normal and $\vec{V} \times \vec{B}$ is zero degrees, a position where the satellite surface is driven most positive by the induced emf. Since the electron current is related exponentially to the surface potential, the sharpness of the current variation near this specific orientation is to be expected.

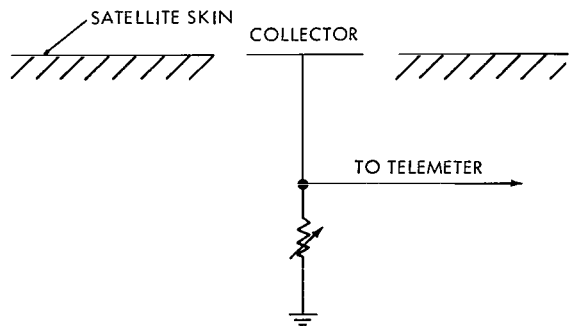


Figure 9—Total current monitor.

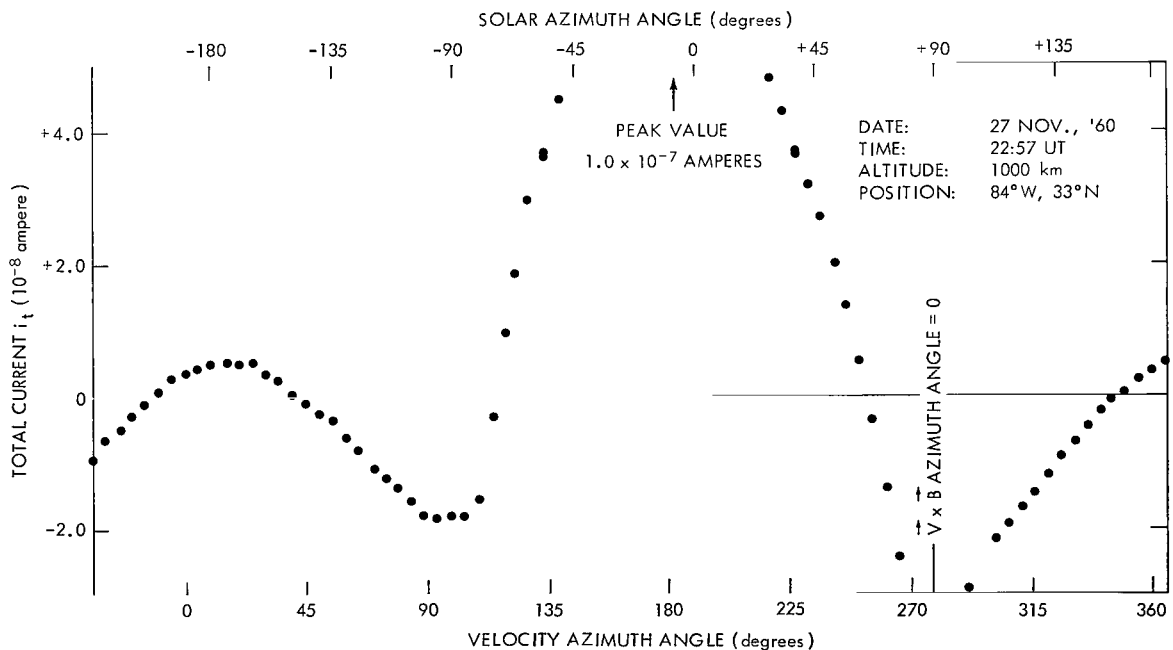


Figure 10—Total current as a function of aspect.

ELIMINATION OF INTERACTION EFFECTS IN DERIVING GEOPHYSICAL PARAMETERS

It is possible from measurements of current flowing to the satellite to extract information on the ambient electron density and temperature and on the ambient ion density and composition. However, the complex behavior of the satellite-plasma interaction, especially short-term variations of satellite potential and unwanted currents require extreme care in so doing. Our methods of deriving geophysical parameters can be described by continuing reference to Figure 10 and the discussion which follows.

To extract the ambient ion concentration, we need to know unambiguously the behavior of i_+ . It is seen from Figure 10 that if we were to use an exposed electrode to determine n_+ , we have the problem of accounting for unwanted masking electron and photocurrents. This is most easily accomplished by experimental separation in the manner illustrated schematically in Figure 3, leading to the easily interpretable result shown in Figure 4. Accurate positive ion densities then are obtainable by use of Equation 7 provided that one precisely knows the angle of attack and provided that ϕ_0 is negative. The latter requirement arises from the fact that a positive satellite potential inhibits positive ions from entering the sensor.

The determination of electron concentration and temperature and of ion composition depends upon a measurement of the electron or ion diffusion current as a function of an applied retarding potential. To accomplish this we must insure that the measured current changes reflect only those due to applied retarding potential. The measurement of ion composition described in the succeeding section was made at the satellite equator. Again, separation of unwanted electron and photocurrents was experimentally accomplished. We next need to account for orientation changes of i_+ . This is accomplished by restricting the reduced data to only that obtained when i_+ is orientation invariant, specifically obtaining a volt-ampere curve when the sensor always was closely pointed into the direction of motion.

Similarly, in extracting the electron parameters we first experimentally separate out the unwanted ion and photocurrents. We feel that this is especially important for charged particle densities less than 10^4 cm^{-3} , since from Figure 10 we know that the unwanted photocurrent can exceed the electron diffusion current even when the satellite is at plasma potential. Once the unwanted currents are separated out, we only need account for orientation changes in the wanted electron diffusion current. With specific reference to Figure 5, it is seen that the electron temperature sensor has two modes of operation. In the first mode, no retarding potential is applied so that the orientation sensitivity illustrated by Figure 6 can be measured. From this knowledge, we then can take that volt-ampere curve in the second mode of operation where the electron diffusion current changes entirely reflect that due to the applied potential.

SUMMARY OF ION COMPOSITION RESULTS

Ion composition was measured on the Explorer VIII satellite by use of a sensor located on the equator and identical to that illustrated in Figure 3 except that a retarding potential was applied in

series with the collector. Previous publications reported that O^+ was the predominant ion at altitudes below 1000 km in the daytime ionosphere (Bourdeau, 1961) and that helium ions become important above this altitude again for the daytime ionosphere (Bourdeau et al., 1962). In this section, we extend the reported results to infer the diurnal upper ionospheric ion composition behavior for the period November-December 1960.

The principle of the experiment (Figure 11) is based on the fact that an ion's kinetic energy (relative to the satellite) is proportional to its mass. In the upper ionosphere, we are concerned principally with three types of ions: O^+ , He^+ and H^+ . Whipple (1959) first set forth the theoretical equations for the volt-ampere behavior of planar ion traps. As illustrated in Figure 11, the shape of this volt-ampere curve is characterized by an inflection point for a binary mixture of O^+ and He^+ and by a plateau for a mixture of O^+ and H^+ . In the illustration, the abscissa is the ion retarding potential, ϕ_r , which is the algebraic sum of the satellite and collector (ϕ_c) potentials. The ordinate is the collector current normalized to that observed at zero retarding potential.

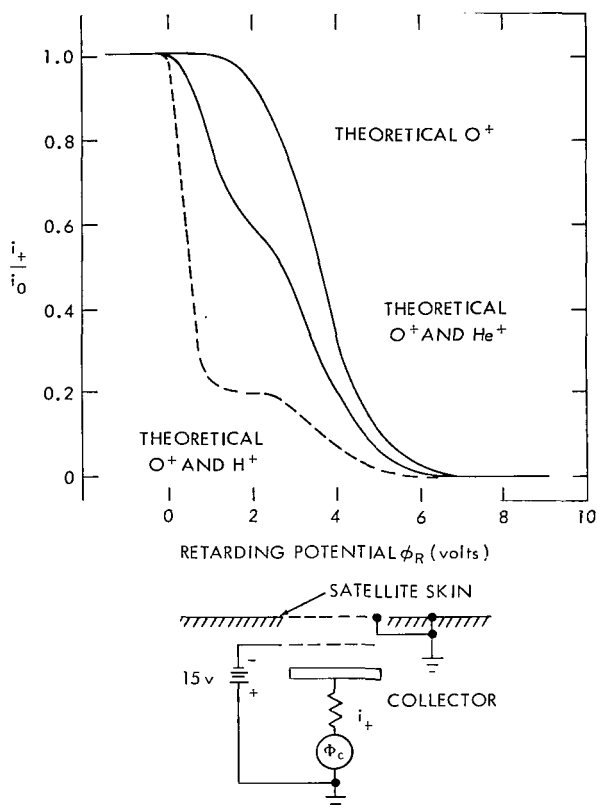


Figure 11—Ion retarding potential experiment.

The diurnal behavior of upper ionospheric composition for the months of November and December 1960, is illustrated in Figure 12. The two upper volt-ampere curves were taken for different altitudes at times which, from the standpoint of the neutral gas temperature represent diurnal minimum conditions. We observe by comparison that (1) the transition altitude where O^+ and He^+ ions had equal concentrations was at about 770 km, and (2) at 980 km the predominant ion was He^+ . In the latter volt-ampere curve, there is slight evidence—from the sharp drop at zero retarding potential—that protons become a trace constituent at 1000 km, so that the transition altitude from He^+ to H^+ would occur at about 1200 km. The lower two curves represent data obtained midway between diurnal minimum and diurnal maximum. We observe from the first that O^+ ions dominated at 800 km and from the second that the O^+ - He^+ transition altitude has risen to 1500 km. We have observed some diurnal maximum data where this transition took place as high as 1800 km. Our daytime volt-ampere curves show no trace of protons.

In summary then, the Explorer VIII retarding potential experiment defines an upper ionosphere where, in late 1960, O^+ ions predominated up to about 800 km at night and up to at least 1500 km

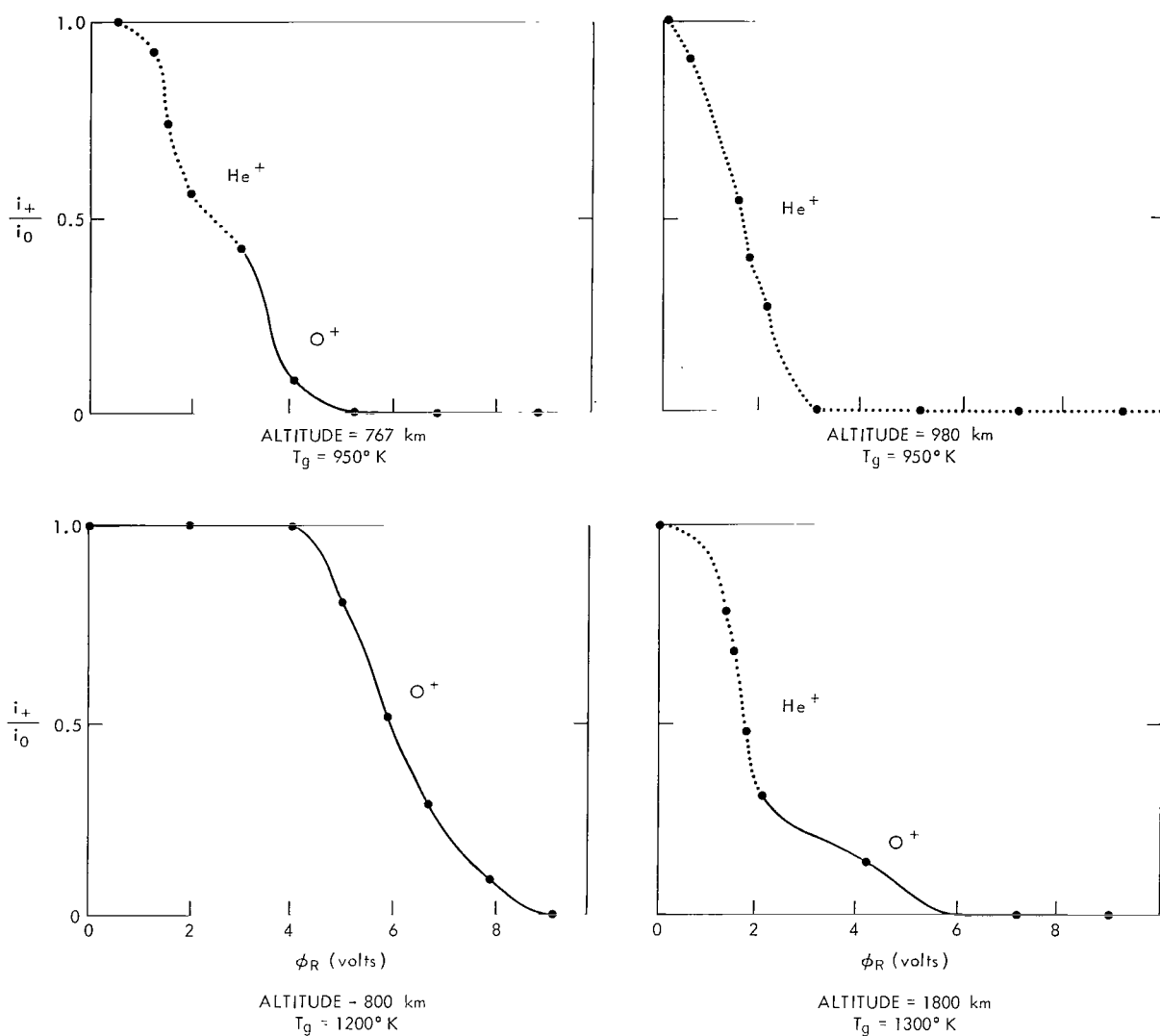


Figure 12—Ion composition results.

during midday. He^+ ions predominated from 800 km to at least 1200 km at night and from 1500 to at least 1800 km at midday. This qualitatively agrees with the theoretical work of Bauer (1963) who postulates that these transition altitudes and thus the thickness of the helium ion region can be related directly to the neutral gas temperature T_g . If we accept a value for T_g of 950°K at the diurnal minimum, then the nighttime Explorer VIII composition results correspond quantitatively to Bauer's theoretical expectation. On the other hand, if we accept current reference atmospheres where the diurnal maximum T_g is given at about 1400°K , then the measured $\text{O}^+ - \text{He}^+$ transition at midday is somewhat higher than in Bauer's model. There is closer agreement with Bauer's model if the daytime electron temperatures discussed in the succeeding section are representative of T_g . The daytime $\text{O}^+ - \text{He}^+$ transition level is somewhat higher than that inferred by Hanson (1962a) from an ion density profile taken at a similar epoch of the solar cycle.

SUMMARY OF ELECTRON TEMPERATURE RESULTS

The Explorer VIII satellite contained two electron temperature probes. The first was the two-electrode device illustrated in Figure 5. In the first of this sensor's two modes of operation, the aperture grid was maintained at spacecraft potential and the device was used to monitor the orientation sensitivity of electron diffusion current, a typical example of which is illustrated in Figure 6. In the second mode, a retarding potential applied to the aperture grid permitted a measurement of satellite potential and of the ambient electron density and temperature. Typical experimental volt-ampere curves for three conditions are illustrated in Figure 13. Electron temperatures are computed from the slope of the exponential portion of the volt-ampere curves. Satellite potential is obtained from the position along the abscissa of the point at which the current departs from its exponential behavior. Electron density is computed from the electron current value taken at this specific retarding potential. The first curve is representative of midnight quiet ionosphere conditions in the 400-600 km region, where values of 900°K , 10^5 cm^{-3} , and -0.75 volt represent typical values of electron temperature and density and satellite potential. The second curve is typical of midday quiet ionosphere conditions at 1000 km where T_e , n_e , and ϕ_s were typically 1600°K , 10^4 cm^{-3} and -0.15 volt. The third curve is typical of midday quiet ionosphere apogee (2400 km) conditions where T_e , n_e , and ϕ_s were typically 1600°K , 10^3 cm^{-3} and $+0.25$ volt.

Although by the method described in previous sections, we have taken into account possible errors in electron temperature determination due to orientation changes of satellite potential and of the three types of exchange currents, there is left a possibility of error due to changes in the aperture grid's electrical transparency with applied potential. This possible error we believe to be small from a comparison of the two-electrode results with a different electron temperature experiment also included on the satellite. Electrically this latter experiment, located near the forward end of the spin axis, was identical to that illustrated in Figure 7 except that an electron retarding potential was applied to the collector. This particular experiment had a poorer telemetry resolution than the two-electrode experiment hence these data were not used extensively. For the times it was used the electron temperature values agreed with those from the two-electrode experiment.

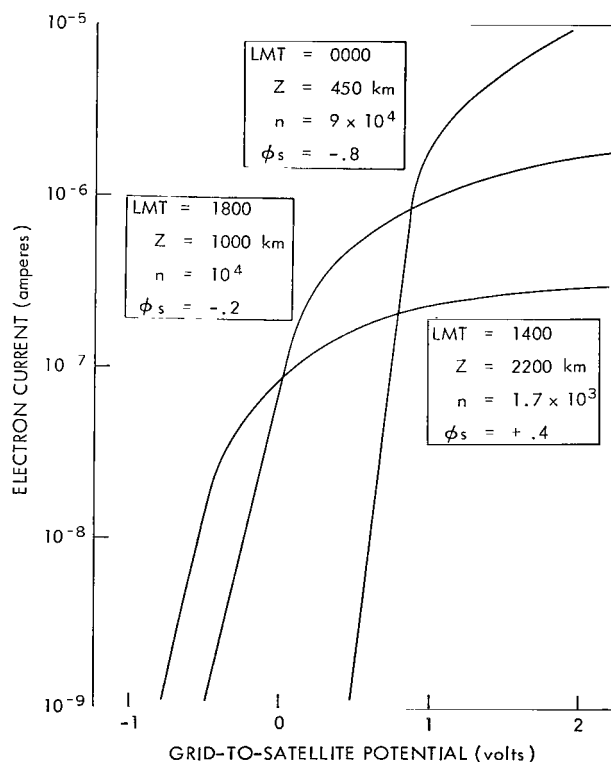


Figure 13—Typical experimental electron temperature volt-ampere curves.

The short active life of the Explorer VIII satellite together with the nature of real time telemetry transmissions severely limits our ability to separate latitude, altitude and diurnal variations of T_e . This problem is made even more difficult because the months of November and December, 1960 were characterized by a number of rather severe solar flares, truly an unfavorable time interval for the proponents of temperature equilibrium between electrons and heavy particles. Accordingly, the presentation of these results has been limited to "quiet" days, specifically when the world wide index (A_p) of magnetic activity was less than 15. The nature of the coverage available from the telemetry receiving network was such that the data apply principally to magnetic dips between 50° and 70° .

The average diurnal variation of T_e taken from approximately one hundred passages over a telemetry station is presented in Figure 14. Also shown is the estimated diurnal variation of the neutral gas temperature in the isothermal altitude region for this level of solar activity, taken from Harris and Priester (1962). There is the need for an immediate note of caution: *we have made the questionable assumption that the electron temperature is independent of altitude*, an assumption

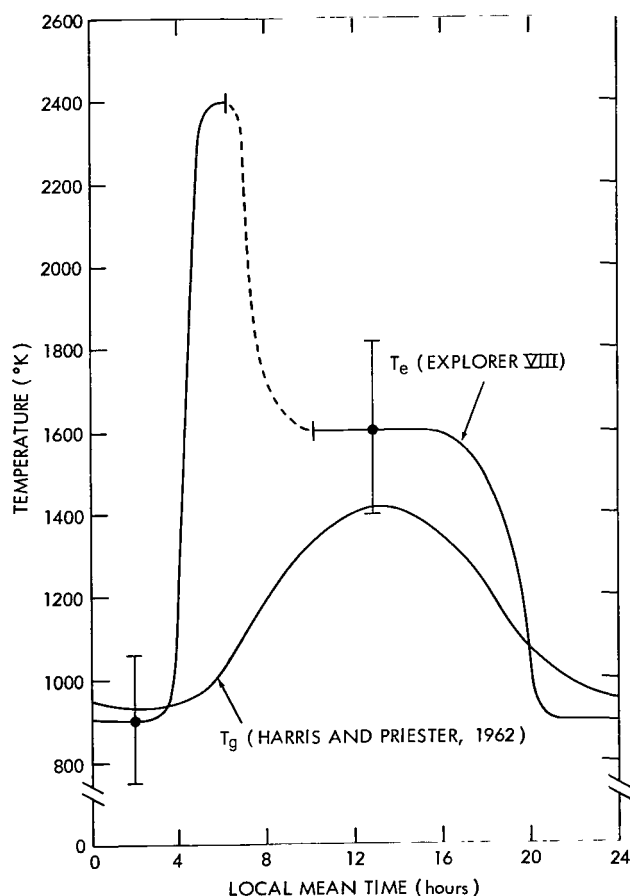


Figure 14—Measured diurnal variation of electron temperature at mid-latitudes for magnetically quiet days ($A_p < 15$).

which can be examined in some detail as the discussion is developed. It is seen, firstly, that the average electron temperature taken during the 6-hour period centered around midnight is 900°K . The individual data points showed a standard deviation of 150°K . Some of this deviation perhaps reflects expected daily variations in the neutral gas temperature. The altitude interval over which these nighttime data apply is 425-600 km. The rocket results of Brace and Spencer (1963) justify the assumption that T_e should be constant with altitude at the diurnal minimum. Our average nighttime value of 900°K is in excellent agreement with estimates of the neutral gas temperature for this epoch of the solar cycle, indicating no nighttime source of ionization for the stated conditions. Although our nighttime values were obtained principally for magnetic dips 50° - 70°N , the little data we have at other latitudes show values that are within the standard deviation at magnetic dips between 0 and 75°N . We did not observe a single value outside this deviation for $A_p < 15$. Our observation that the nighttime electron temperature is consonant with the neutral gas temperature contrasts with the midnight rocket result obtained at a magnetic dip of 70°N , for low geomagnetic activity by

Brace and Spencer (1963). Their value of about 1200°K was obtained in December 1961 when the estimated T_g was about 800°, thus suggesting a ratio of T_e/T_g of 1.5. We tend not to ascribe the different spaceflight results to the different experimental approaches used since, as discussed later, the Explorer VIII midday results are in harmony with those of Brace and Spencer. They ascribe their high nighttime value to the possible existence of a local ionization source. Alouette satellite results obtained in late 1962 (Knecht and Van Zandt, 1963) show that spread-F conditions are a characteristic feature of the upper ionosphere about 70° magnetic dip. This feature also probably is related to the existence of a secondary ionization source. Willmore et al. (1962) in their preliminary analysis of Ariel satellite results (which also supposes that T_e is independent of altitude) report a latitude dependence of nighttime electron temperature with a spread that lies just outside our standard deviation. Their high latitude values are significantly above the neutral gas temperature inferred from current reference atmospheres. The most probable means of accommodating the Explorer VIII nighttime results with these other spaceflight observations is to suggest a nighttime ionization source at high magnetic dips which grows in relative importance as one approaches the year of minimum solar activity.

Turning now to the midday 6-hour period centered at 1300 LMT, the average observed electron temperature for this time interval was 1600°K with a standard deviation of 200°K. This portion of the diurnal variation was obtained at altitudes between 1000-2000 km and mostly over Australia (magnetic dip 50-70°S). We have not included in this average a few percent of the total number of observations where anomalously high values were observed. These could represent residual effects of solar flares which characterized the active life of Explorer VIII. The average value of 1600°K is within 200°K of current estimates of the neutral gas temperature at diurnal maximum for the period November-December 1960. Our average value agrees well with other spaceflight results obtained for the same latitude, similarly "quiet" ionospheric conditions and during the same epoch of the solar cycle. Hanson (1962) infers from an ion density profile taken in October 1960 that $(T_e + T_i)/2$ was 1600°K, data which apply to our altitude interval. When Hanson's result is compared with the Explorer VIII T_e result, we conclude that $T_e \approx T_i$ for this general time interval and in this altitude region. We also infer close equivalency of the charged particle and neutral gas temperatures. Assuming altitude-independent temperatures, the Explorer VIII result also is in good agreement with the value for $(T_e + T_i)/2$ of 1600°K obtained in the altitude region 350-600 km by Jackson and Bauer (1961) from an electron density profile measured on a rocket launched in April 1961. Again assuming altitude-independent temperatures, we also are in good agreement with the March 1961 rocket measurement of T_e obtained at about 350 km by Brace and Spencer (1963) who conclude: "...thermal equilibrium is normal in the quiet, daytime ionosphere at mid-latitude, except in the lower F-region (approximately 150-300 km)."

We emphasize that all of the above described rocket results and the conclusion of temperature equilibrium derived therefrom were obtained at midday, at mid-latitudes under quiet ionospheric conditions and for a specific epoch of the solar cycle. *Evidence is growing that to generalize the conclusion of temperature equilibrium for all latitudes and for other portions of the solar cycles would be premature.* Brace and Spencer (1963) report high electron temperatures in the auroral region during 1960. Evans (1962) reports a value for T_e/T_i of 1.6 above 200 km obtained in 1962

at magnetic dip 70°N from ground-based incoherent backscatter observations. The reported high-latitude midday T_e results from the Ariel satellite (Willmore et al., 1962) have values significantly higher than the estimated neutral gas temperature for the pertinent time interval (May 1962). Since some of these data were obtained at the quoted Explorer VIII latitudes, there is an inference that the ratio T_e/T_i tends to increase considerably both as we approach solar minimum and/or go to high latitudes.

We consider last the most pronounced feature of the Explorer VIII diurnal T_e variation—the high electron temperatures observed in the sunrise period. These values of up to 2.5 times the estimated neutral gas temperature were obtained in the altitude interval 600–900 km at magnetic dips 50° – 70° . Bowles et al. (1962) report a maximum in T_e/T_i during the sunrise period from ground-based incoherent backscatter results obtained at the geomagnetic equator. Evans (1962), on the other hand, reports that T_e/T_i reaches a maximum at noon. Hanson (1962b) and Dalgarno et al. (1962) on the assumptions that solar radiation is the only ionizing source and that the excess photoelectron energy is deposited below the F2 peak have estimated theoretically small differences

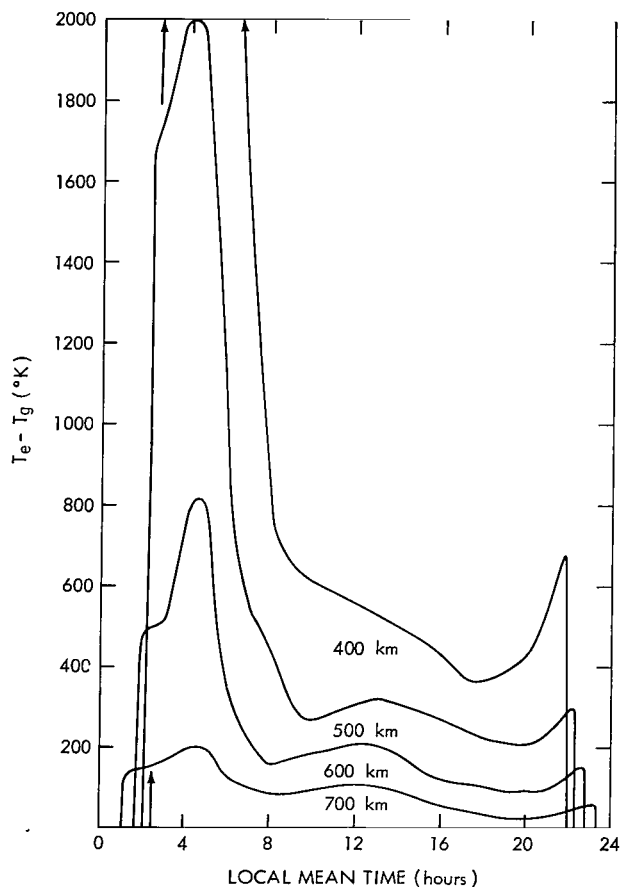


Figure 15—Qualitative diurnal variation of difference between electron and ion temperatures, predicted from diurnal variation of $n(\text{O})$ and n_e .

in T_e and T_i in the upper ionosphere but only for a midday ionosphere. Both works relate the temperature difference $(T_e - T_i)$ for altitudes above the F2 peak to the ratio $n(\text{O})/n_e^2$ where $n(\text{O})$ is the number density of oxygen atoms. Dalgarno (1963) using hypothetical values for n_e has extended the theoretical estimates to suggest high electron temperatures in the sunrise period. We have applied this reasoning to a more practical case by dividing the diurnal variation of $n(\text{O})$ given by Harris and Priester (1962) by the diurnal n_e^2 variation reported by Blumle et al. (1963) from the Alouette satellite, both variations applying to the period of late 1962. The result for different altitude increments is presented in Figure 15. It shows that high electron temperatures should be expected in the sunrise period but that the effect becomes rather diffuse at altitudes above 700 km. It additionally shows that the temperature difference can increase somewhat in the sunset period. We emphasize the qualitative nature of Figure 15 principally because (1) the solar ultraviolet intensity was not measured at the same time and (2) $n(\text{O})$ is an inferred rather than a measured parameter. However if the shape of the $n(\text{O})$ variation as a function of diurnal time is correct, we would expect T_e/T_i to

be largest at sunrise and increase somewhat at sunset for the altitude interval of the Explorer VIII measurements. We do observe that T_e is a maximum at sunrise and that T_e/T_i is somewhat larger at sunset than at midday. The sunset data shown in Figure 13 were obtained between 600-900 km. We did not include in this averaging several higher altitude observations where T_e was higher than the average curve. Hanson (1962b) has suggested the possibility that some photoelectrons can diffuse along magnetic field lines and deposit their energy at higher altitudes. This would be critically dependent on the relationship between magnetic dip and the solar zenith angle. It is possible that the higher T_e values observed above 900 km at sunset are related to this hypothesis.

(Manuscript received August 8, 1963)

REFERENCES

- Bauer, S. J., "Helium Belt in the Upper Atmosphere," *Nature* 197:36-37, January 5, 1963.
- Blumle, L. J., Fitzenreiter, R. J., Bauer, S. J., and Jackson, J. E., "Diurnal Variations of the Topside Ionosphere at Mid-latitudes," presentation at 44th Annual Meeting of the American Geophysical Union, Washington, D. C., April 18, 1963.
- Bourdeau, R. E., "Ionospheric Results with Sounding Rockets and the Explorer VIII Satellite," In: *Space Research II; Proc. 2nd Internat. Space Sci. Symp., Florence, Apr. 10-14, 1961*, Amsterdam: North-Holland Publishing Co., 1961, pp. 554-573.
- Bourdeau, R. E., Donley, J. L., Serbu, G. P., and Whipple, E. C., Jr., "Measurements of Sheath Currents and Equilibrium Potential on the Explorer VIII Satellite," *J. Astronaut. Sci.* 8(3):65-73, 1961.
- Bourdeau, R. E., Whipple, E. C., Jr., Donley, J. L., and Bauer, S. J., "Experimental Evidence for the Presence of Helium Ions Based on Explorer VIII Satellite Data," *J. Geophys. Res.* 67(2):467-476, February 1962.
- Bowles, K. L., Ochs, G. R., and Green, J. L., "On the Absolute Intensity of Incoherent Scatter Echoes from the Ionosphere," *J. Res. Nat. Bur. Stand. (D. Rad. Prop.)* 66D(4):395-407, July-August 1962.
- Brace, L. H., Spencer, N. W., and Corrigan, G. R., "Ionosphere Electron Temperature Measurements and their Implications," *J. Geophys. Res.* 68(19):5397-5412, October 1, 1963.
- Donley, J. L., "Experimental Evidence for a Low Ion-Transition Altitude in the Upper Nighttime Ionosphere," *J. Geophys. Res.* 68(7):2058-2060, April 1, 1963.
- Evans, J. V., "Diurnal Variation of the Temperature of the F Region," *J. Geophys. Res.* 67(12):4914-4920, November 1962.
- Gringauz, K. I., and Zelikman, M. Kh., "Measurement of the Positive Ion Density Along the Orbit of an Artificial Earth Satellite," *Uspekhi Fiz. Nauk*, 63(1b):239-252, 1957 (In Russian).
- Hanson, W. B., "Upper Atmosphere Helium Ions," *J. Geophys. Res.* 67(1):183-188, January 1962.
- Harris, I., and Priester, W., "Theoretical Models for the Solar-Cycle Variation of the Upper Atmosphere," *J. Geophys. Res.* 67(12):4585-4591, November 1962.

- Hinteregger, H. E., Damon, K. R., and Hall, L. H., "Analysis of Photoelectrons from Solar Extreme Ultraviolet," *J. Geophys. Res.* 64(8):961-969, August 1959.
- Jackson, J. E., and Bauer, S. J., "Rocket Measurement of a Day-time Electron-Density Profile up to 620 Kilometers," *J. Geophys. Res.* 66(9):3055-3057, September 1961.
- Knecht, R. W., and Van Zandt, T. E., "Some Early Results from the Ionospheric Topside Sounder Satellite," *Nature* 197(4868):641-644, February 16, 1963.
- Krassovsky, V. I., "Exploration of the Upper Atmosphere with the Help of the Third Soviet Sputnik," *Proc. I.R.E.* 47(2):289-296, February 1959.
- Schulz, G. J., and Brown, S. C., "Microwave Study of Positive Ion Collection by Probes," *Phys. Res.* 98(6):1642-1649, June 15, 1955.
- Serbu, G. P., Bourdeau, R. E., and Donely, J. L., "Electron Temperature Measurements on the Explorer VIII Satellite," *J. Geophys. Res.* 66(12):4313-4315, 1961.
- Whale, H. A., "The Excitation of Electroacoustic Waves by Antennas in the Ionosphere," *J. Geophys. Res.* 68(2):415-422, January 15, 1963.
- Whipple, E. C., Jr., "The Ion-Trap Results in 'Exploration of the Upper Atmosphere with the Help of the Third Soviet Sputnik'," *Proc. I.R.E.* 47(11):2023-2024, November 1959.

2/7/85
87

"The aeronautical and space activities of the United States shall be conducted so as to contribute . . . to the expansion of human knowledge of phenomena in the atmosphere and space. The Administration shall provide for the widest practicable and appropriate dissemination of information concerning its activities and the results thereof."

—NATIONAL AERONAUTICS AND SPACE ACT OF 1958

NASA SCIENTIFIC AND TECHNICAL PUBLICATIONS

TECHNICAL REPORTS: Scientific and technical information considered important, complete, and a lasting contribution to existing knowledge.

TECHNICAL NOTES: Information less broad in scope but nevertheless of importance as a contribution to existing knowledge.

TECHNICAL MEMORANDUMS: Information receiving limited distribution because of preliminary data, security classification, or other reasons.

CONTRACTOR REPORTS: Technical information generated in connection with a NASA contract or grant and released under NASA auspices.

TECHNICAL TRANSLATIONS: Information published in a foreign language considered to merit NASA distribution in English.

TECHNICAL REPRINTS: Information derived from NASA activities and initially published in the form of journal articles.

SPECIAL PUBLICATIONS: Information derived from or of value to NASA activities but not necessarily reporting the results of individual NASA-programmed scientific efforts. Publications include conference proceedings, monographs, data compilations, handbooks, sourcebooks, and special bibliographies.

Details on the availability of these publications may be obtained from:

SCIENTIFIC AND TECHNICAL INFORMATION DIVISION
NATIONAL AERONAUTICS AND SPACE ADMINISTRATION
Washington, D.C. 20546